

Production of $f_0(980)$ meson at the LHC: Color evaporation versus color-singlet gluon-gluon fusion

Piotr Lebiedowicz,^{1,*} Rafał Maciuła,^{1,†} and Antoni Szczurek ^{c1,§}

¹*Institute of Nuclear Physics Polish Academy of Sciences,
ul. Radzikowskiego 152, PL-31342 Kraków, Poland*

Abstract

The production of the $f_0(980)$ meson at high energies is not well understood. We investigate two different potential mechanisms for inclusive scalar meson production in the k_t -factorization approach: color-singlet gluon-gluon fusion and color evaporation model. The $\gamma^*\gamma^* \rightarrow f_0(980)$ form factor(s) can be constraint from the $f_0(980)$ radiative decay width. The $g^*g^* \rightarrow f_0(980)$ form factors are obtained by a replacement of α_{em} electromagnetic coupling constant by α_s strong coupling constant and appropriate color factors. The form factors for the two couplings are parametrized with a function motivated by recent results for scalar quarkonia. The differential cross sections are calculated in the k_t -factorization approach with modern unintegrated gluon distributions. Unlike for quarkonia it seems rather difficult to describe a preliminary ALICE data for inclusive production of $f_0(980)$ exclusively by the color singlet gluon-gluon fusion mechanism. Two different scenarios for flavor structure of $f_0(980)$ are considered in this context. We consider also mechanism of fusion of quark-antiquark associated with soft gluon emission in a phenomenological color evaporation model (CEM) used sometimes for quarkonium production. Here we use k_t -factorization version of CEM to include higher-order contributions. In addition, for comparison we consider also NLO collinear approach with $q\bar{q}q$ and $q\bar{q}g$ color octet partonic final states. Both approaches lead to a similar result. However, very large probabilities are required to describe the preliminary ALICE data. The pomeron-pomeron fusion mechanism is also discussed and results are quantified.

^c Also at *College of Natural Sciences, Institute of Physics, University of Rzeszów, ul. Pigonia 1, PL-35310 Rzeszów, Poland.*

^{*} Piotr.Lebiedowicz@ifj.edu.pl

[†] Rafal.Maciula@ifj.edu.pl

[§] Antoni.Szczurek@ifj.edu.pl

I. INTRODUCTION

The production of light mesons in high-energy proton-proton collisions is rather poorly understood. Representative examples are production of $f_0(500)$, $\rho(770)$, $f_0(980)$ or $f_2(1270)$. Parallel we discussed inclusive production of $f_2(1270)$ meson in proton-proton collisions [1] where it is found that the preliminary ALICE data [2] can be almost explained at higher $f_2(1270)$ transverse momentum ($p_t > 3$ GeV) using color-singlet gluon-gluon fusion mechanism. The $f_2(1270)$ meson is usually considered to have a $\frac{1}{\sqrt{2}}(u\bar{u} + d\bar{d})$ flavor structure. Here we wish to explore the situation for the production of a rather enigmatic $f_0(980)$.

In general, light scalar mesons are poorly understood [3]. In particular, it is not clear whether they are of the $q\bar{q}$ character or are tetraquarks [4]. Most mesons are thought to be formed from combinations of $q\bar{q}$. In the literature, the hadronic structure of the $f_0(980)$ meson has been discussed for decades and there are many different interpretations, from the conventional $q\bar{q}$ picture [5, 6] to multiquark [7, 8] or $K\bar{K}$ bound states [9–12]. Some authors introduce the concept of $qq\bar{q}\bar{q}$ states [4] or even superpositions of the tetraquark state with the $q\bar{q}$ state [13, 14]. The structure of $f_0(980)$ can be studied also in nonsemileptonic decays of D, D_s mesons [15] or B, B_s mesons [16, 17].

Note that $f_0(980)$ state was seen in both $\pi\pi$ and $K\bar{K}$ channel [18] with a considerable branching fraction. For the branching ratios see the discussion, e.g., in Refs. [14, 19].

In the present letter we investigate whether the gluon-gluon fusion or color evaporation approaches known from quarkonium production can explain the new preliminary ALICE data [2]. As this is a first analysis on the subject we shall consider a simple $q\bar{q}$ structure of $f_0(980)$ meson. We shall consider different flavor combinations. This has of course important consequences for $\gamma^*\gamma^* \rightarrow f_0(980)$ coupling due to charges of quarks/antiquarks. Such couplings are important ingredients for calculating $f_0(980)$ contribution to light-by-light component to anomalous magnetic moment of the muon [20–22]. In Ref. [23] it was argued that $f_0(980)$ must be dominantly $s\bar{s}$ to describe radiative decay $\phi \rightarrow f_0(980)\gamma$. This is dictated by the fact that $\Gamma(\phi \rightarrow f_0(980)\gamma) \gg \Gamma(\phi \rightarrow a_0(980)\gamma)$. In Ref. [24] the $\gamma^* - f_0(980)$ transition form factor was studied assuming the simple $s\bar{s}$ structure. Only F_{TT} transverse form factor was included in this analysis. The role of F_{LL} longitudinal form factor was not studied so far.

II. SOME DETAILS OF THE MODEL CALCULATIONS

A. The $\gamma^*\gamma^* \rightarrow f_0(980)$ fusion process

In the formalism presented e.g. in [25] the covariant matrix element for the $\gamma^*\gamma^* \rightarrow f_0(980)$ process is written as:

$$\begin{aligned} \mathcal{M}^{\mu\nu} = 4\pi\alpha_{\text{em}} \frac{v}{m_{f_0}} & \left[-R^{\mu\nu}(q_1, q_2) F_{TT}(Q_1^2, Q_2^2) \right. \\ & \left. + \frac{v}{X} \left(q_1^\mu + \frac{Q_1^2}{v} q_2^\mu \right) \left(q_2^\nu + \frac{Q_2^2}{v} q_1^\nu \right) F_{LL}(Q_1^2, Q_2^2) \right], \end{aligned} \quad (2.1)$$

where $\nu = (q_1 \cdot q_2)$, $X = \nu^2 - q_1^2 q_2^2$, and

$$R^{\mu\nu}(q_1, q_2) = -g^{\mu\nu} + \frac{1}{X} \left[\nu (q_1^\mu q_2^\nu + q_2^\mu q_1^\nu) - q_1^2 q_2^\mu q_2^\nu - q_2^2 q_1^\mu q_1^\nu \right]. \quad (2.2)$$

Here q_1 and q_2 denote the momenta of the photons, $Q_1^2 = -q_1^2$, $Q_2^2 = -q_2^2$, and m_{f_0} is mass of the $f_0(980)$ meson. In Eq. (2.1), the scalar meson structure information is encoded in the form factors F_{TT} and F_{LL} which are functions of the virtualities of both photons. F_{TT} or F_{LL} correspond to the situation where either both photons are transverse or longitudinal, respectively. By definition the form factors are dimensionless.

For scalar quarkonium states a microscopic calculation is reliable; see [26]. For light mesons the situation is more complicated. Here we will try to rather parametrize the form factors.

The two-photon decay width of the $f_0(980)$ meson can be calculated as:

$$\Gamma(f_0(980) \rightarrow \gamma\gamma) = \frac{\pi\alpha_{\text{em}}^2}{4} m_{f_0} |F_{TT}(0,0)|^2. \quad (2.3)$$

Only F_{TT} form factor can be constraint from (2.3). The radiative decay width is relatively well known, see [18]. Using the average decay width quoted in [18]

$$\Gamma(f_0(980) \rightarrow \gamma\gamma) = 0.31 \text{ keV}, \quad (2.4)$$

and $m_{f_0} = 980 \text{ MeV}$ we obtain from (2.3) $|F_{TT}(0,0)| = 0.087$. Then the transverse form factor is parametrized as:

$$\frac{F_{TT}(Q_1^2, Q_2^2)}{F_{TT}(0,0)} = \left(\frac{\Lambda_M^2}{Q_1^2 + Q_2^2 + \Lambda_M^2} \right), \quad (2.5)$$

$$\frac{F_{TT}(Q_1^2, Q_2^2)}{F_{TT}(0,0)} = \left(\frac{\Lambda_D^2}{Q_1^2 + Q_2^2 + \Lambda_D^2} \right)^2, \quad (2.6)$$

where cut-off parameters Λ_M or Λ_D are expected to be of order of 1 GeV. Both monopole (2.5) and dipole (2.6) parametrizations of F_{TT} will be used in the following. In the calculations we take $\Lambda_M = \Lambda_D = m_{f_0}$.

The F_{LL} form factor is rather unknown but via construction do not enter the formula for the radiative decay width (2.3) as

$$F_{LL}(0, Q_2^2) = F_{LL}(Q_1^2, 0) = 0. \quad (2.7)$$

We propose to use the following parametrization for the F_{LL} form factor:

$$F_{LL}(Q_1^2, Q_2^2) = R_{LL/TT} \frac{Q_1^2}{M_0^2 + Q_1^2} \frac{Q_2^2}{M_0^2 + Q_2^2} F_{TT}(Q_1^2, Q_2^2). \quad (2.8)$$

Such a form is consistent with a microscopic calculation for $\gamma^* \gamma^* \rightarrow \chi_{c0}$ [26] using quarkonium wave functions obtained from the potential models. In our present case we expect $R_{LL/TT} \approx \pm 0.5$ and $M_0 \sim m_{f_0}$.

B. Color singlet $g^*g^* \rightarrow f_0(980)$ fusion

In Fig. 1 we show a generic Feynman diagram for $f_0(980)$ meson production in proton-proton collision via gluon-gluon fusion. This diagram illustrates the situation adequate for the k_t -factorization calculations used in the present paper.

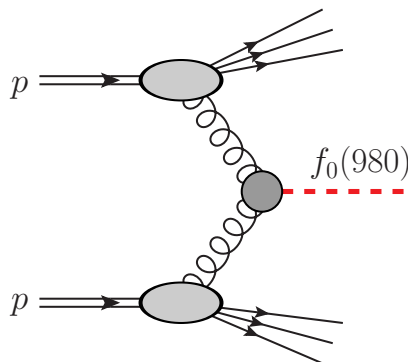


FIG. 1. General diagram for inclusive $f_0(980)$ production via gluon-gluon fusion in proton-proton collisions.

The differential cross section for inclusive $f_0(980)$ meson production via the $g^*g^* \rightarrow f_0(980)$ fusion in the k_t -factorization approach can be written as:

$$\frac{d\sigma}{dyd^2\mathbf{p}} = \int \frac{d^2\mathbf{q}_1}{\pi q_1^2} \mathcal{F}_g(x_1, \mathbf{q}_1^2) \int \frac{d^2\mathbf{q}_2}{\pi q_2^2} \mathcal{F}_g(x_2, \mathbf{q}_2^2) \delta^{(2)}(\mathbf{q}_1 + \mathbf{q}_2 - \mathbf{p}) \frac{\pi}{(x_1 x_2 s)^2} \overline{|\mathcal{M}|^2}. \quad (2.9)$$

Here \mathbf{q}_1 , \mathbf{q}_2 and \mathbf{p} denote the transverse momenta of the gluons and the $f_0(980)$ meson. $\mathcal{M}_{g^*g^* \rightarrow f_0}$ is the off-shell matrix element for the hard subprocess and \mathcal{F}_g are the gluon unintegrated distribution functions (UGDFs) for both colliding protons. The UGDFs depend on gluon longitudinal momentum fractions $x_{1,2} = m_T \exp(\pm y) / \sqrt{s}$ and $\mathbf{q}_1^2, \mathbf{q}_2^2$ entering the hard process. In principle, they can depend also on factorization scales $\mu_{F,i}^2$, $i = 1, 2$. It is reasonable to assume $\mu_{F,1}^2 = \mu_{F,2}^2 = m_T^2$. Here m_T is transverse mass of the produced $f_0(980)$ meson; $m_T = \sqrt{\mathbf{p}^2 + m_{f_0}^2}$. The $\delta^{(2)}$ function in Eq. (2.9) can be easily eliminated by introducing $\mathbf{q}_1 + \mathbf{q}_2$ and $\mathbf{q}_1 - \mathbf{q}_2$ transverse momenta [27].

The off-shell matrix element can be written as (we restore the color indices a and b)

$$\mathcal{M}^{ab} = \frac{q_{1t}^\mu q_{2t}^\nu}{|\mathbf{q}_1||\mathbf{q}_2|} \mathcal{M}_{\mu\nu}^{ab} = \frac{q_{1+} q_{2-}}{|\mathbf{q}_1||\mathbf{q}_2|} n^{+\mu} n^{-\nu} \mathcal{M}_{\mu\nu}^{ab} = \frac{x_1 x_2 s}{2|\mathbf{q}_1||\mathbf{q}_2|} n^{+\mu} n^{-\nu} \mathcal{M}_{\mu\nu}^{ab} \quad (2.10)$$

with the lightcone components of gluon momenta $q_{1+} = x_1 \sqrt{s/2}$, $q_{2-} = x_2 \sqrt{s/2}$.

The $g^*g^* \rightarrow f_0(980)$ coupling entering in the matrix element squared can be obtained from that for $\gamma^*\gamma^* \rightarrow f_0(980)$ coupling (see e.g. [28]) by the following replacement:

$$\alpha_{\text{em}}^2 \rightarrow \alpha_s^2 \frac{1}{4N_c(N_c^2 - 1)} \frac{1}{(\langle e_q^2 \rangle)^2}. \quad (2.11)$$

($\langle e_q^2 \rangle$) above strongly depends on the flavor structure of the wave function. In the following we consider a few examples of quark-flavor composition:

- $|f_0(980)\rangle = \frac{1}{\sqrt{2}} (|u\bar{u}\rangle + |d\bar{d}\rangle) ,$ (2.12)

- $|f_0(980)\rangle = |s\bar{s}\rangle ,$ (2.13)

- $|f_0(980)\rangle = \frac{1}{\sqrt{2}} (|[su][\bar{s}\bar{u}]\rangle + |[sd][\bar{s}\bar{d}]\rangle) .$ (2.14)

The first function is written in analogy to the rather well known flavor wave function of $f_2(1270)$ meson. The second function was suggested by analysis of radiative decays of ϕ meson as discussed in the introduction. The last function (tetraquark) is supported by spectroscopy of scalar mesons (see e.g. [4]). The scalar mesons with masses below 1 GeV can be understood to be of the tetraquark character and those above 1 GeV as of the $q\bar{q}$ or glueball character. There is, however, no general consensus and the situation is open in our opinion. To reach final picture one must include very different processes simultaneously.

In realistic calculations the running of strong coupling constants must be included. In our numerical calculations presented below, we set the factorization scale to $\mu_F^2 = m_T^2$, and the renormalization scale is taken in the form:

$$\alpha_s^2 \rightarrow \alpha_s(\max\{m_T^2, q_1^2\}) \alpha_s(\max\{m_T^2, q_2^2\}) .$$
 (2.15)

C. Color evaporation model (CEM)

The general diagram representing the color evaporation model (CEM) [29, 30] is shown in Fig. 2. In this approach one uses the perturbative calculation of $q\bar{q}$ minijets.

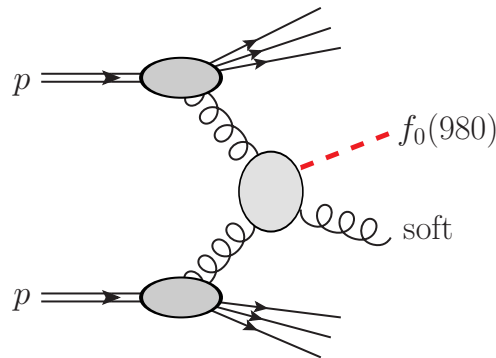


FIG. 2. General diagram for inclusive $f_0(980)$ production in proton-proton collisions in the color evaporation approach.

Fig. 3 represents diagram with $q\bar{q}$ production in the k_t -factorization approach in proton-proton collisions. Here, we calculate $u\bar{u}$ and $d\bar{d}$ production, or alternatively $s\bar{s}$ production, in a similar way as it was done for $c\bar{c}$ production [31]. The color of the $u\bar{u}$

or $d\bar{d}$ is typically in the octet representation. The further emissions of soft gluons are not explicit but will be contained in a multiplicative factor P_{CEM} defined below.

Everything is contained in a suitable renormalization of the $q\bar{q}$ -cross section when integrating over certain limits in the $q\bar{q}$ invariant mass. Having calculated differential cross section for $q\bar{q}$ -pair production one can obtain the cross section for $f_0(980)$ meson within the framework of the CEM. The $q\bar{q} \rightarrow f_0(980)$ transition can be formally written as follows:

$$\frac{d\sigma_{f_0}(p_{f_0})}{d^3p_{f_0}} = P_{\text{CEM}} \int_{m_{f_0}-\Delta M}^{m_{f_0}+\Delta M} d^3P_{q\bar{q}} dM_{q\bar{q}} \frac{d\sigma_{q\bar{q}}(M_{q\bar{q}}, P_{q\bar{q}})}{dM_{q\bar{q}} d^3P_{q\bar{q}}} \delta^3\left(\vec{p}_{f_0} - \frac{m_{f_0}}{M_{q\bar{q}}} \vec{P}_{q\bar{q}}\right), \quad (2.16)$$

where P_{CEM} is the probability of the $q\bar{q} \rightarrow f_0(980)$ transition which is fitted to the experimental data, $M_{q\bar{q}}$ and $P_{q\bar{q}} = |\vec{P}_{q\bar{q}}|$ are the invariant mass and momentum of the $q\bar{q}$ system. Here we take $\Delta M = 100$ MeV.

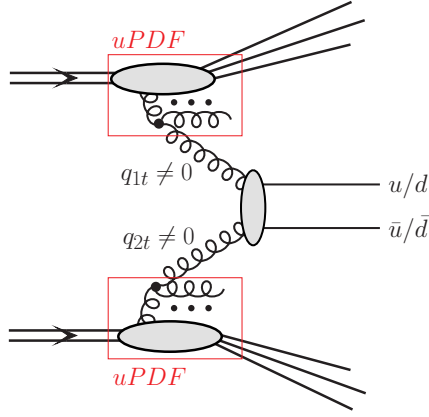


FIG. 3. Typical k_t -factorization process with the production of $u\bar{u}$ and $d\bar{d}$ pairs that are intermediate state for color evaporation.

In Fig.4 we show an example of the diagram relevant for collinear next-to-leading order approach. A full list of processes included in the calculation will be presented in the result section. Within the collinear-factorization approach in the leading-order (LO) approximation, the transverse momentum of the $q\bar{q}$ pair is equal to zero. In fact, the NLO diagrams for the inclusive minijets, such as $gg \rightarrow gq\bar{q}$ or $qg \rightarrow qq\bar{q}$, constitute the LO contributions for the $q\bar{q}$ -pair transverse momentum. Similarly, the next-to-next-to-leading-order (NNLO) topologies for this quantity are effectively NLO. The situation is different in the k_t -factorization approach where nonzero $q\bar{q}$ -pair transverse momentum can be obtained already at leading order within the $g^*g^* \rightarrow q\bar{q}$ and $q^*\bar{q}^* \rightarrow q\bar{q}$ mechanisms.

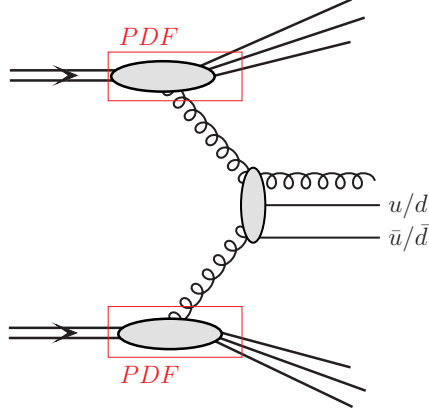


FIG. 4. An alternative collinear approach with the production of $u\bar{u}$ and $d\bar{d}$ pairs associated with soft gluon emission that are intermediate state for color evaporation.

III. NUMERICAL RESULTS

In this section we will present results for the color-singlet gluon-gluon fusion and color evaporation model.

To convert to the number of $f_0(980)$ mesons per event, as was presented in Ref. [2], we use the following relation:

$$\frac{dN}{dp_t} = \frac{1}{\sigma_{\text{inel}}} \frac{d\sigma}{dp_t}. \quad (3.1)$$

The inelastic cross section for $\sqrt{s} = 7$ TeV was measured at the LHC and is:

$$\sigma_{\text{inel}} = 73.15 \pm 1.26 \text{ (syst.) mb}, \quad (3.2)$$

$$\sigma_{\text{inel}} = 71.34 \pm 0.36 \text{ (stat.)} \pm 0.83 \text{ (syst.) mb}, \quad (3.3)$$

as obtained by the TOTEM [32] and ATLAS [33] collaborations, respectively. In our calculations we take $\sigma_{\text{inel}} = 72.5$ mb.

A. Gluon-gluon fusion

As discussed in the previous section the result of the color-singlet gluon-gluon fusion strongly depends on the flavor structure of $f_0(980)$ which is related to the $(\langle e_q^2 \rangle)^2$ in Eq. (2.11). For example $(\langle e_q^2 \rangle)^2 = 25/162$ for first scenario (2.12), $(\langle e_q^2 \rangle)^2 = 1/81$ for the $s\bar{s}$ scenario (2.13). For the tetraquark scenario $(\langle e_q^2 \rangle)^2 = 1/162$ (2.14) assuming diquark as elementary object, but everything depends on details and assumptions made for diquark.

In Fig. 5 we present the $f_0(980)$ meson transverse momentum distributions at $\sqrt{s} = 7$ TeV and $|y| < 0.5$. Here we show results for the color-singlet gluon-gluon fusion contribution for the $s\bar{s}$ scenario for two different UGDFs, JH UGDF (left panel) and KMR UGDF (right panel) together with the preliminary ALICE data from [2]. These UGDFs are available from the CASCADE Monte Carlo code [34]:

- We use a glue constructed according to the prescription initiated in [35] and later updated in [36, 37], which we label as “KMR UGDF”.
- The second type of UGD which we use has been obtained by Hautmann and Jung [38] from a description of precise HERA data on deep inelastic structure function by a solution of the CCFM evolution equation [39–41]. We use “JH-2013-set2” of Ref. [38], which we label as “JH UGDF”.

We show results for the monopole (2.5) and dipole (2.6) form factors with the cut-off parameter $\Lambda_M = \Lambda_D = m_{f_0}$. For the LL form factor (2.8) we take $R_{LL/TT} = \pm 0.5$. The upper solid lines are for $R_{LL/TT} = -0.5$ while the bottom lines for 0.5. The JH UGDF (see the left panel) gives slightly larger cross section than the KMR UGDF (see the right panel). The theoretical distribution for the monopole form factor with $\Lambda_M = m_{f_0}$ exceeds the ALICE data for $p_t > 2$ GeV.

The obtained results are much below the preliminary ALICE data [2] at low $f_0(980)$ transverse momenta. Does it mean that other mechanism(s) is (are) at the game?

It seems that even the $s\bar{s}$ scenario does not allow to describe the ALICE data. A big gluonic component in the $f_0(980)$ wave function could help to improve the situation. Large $K\bar{K}$ molecular component could be another solution.

In addition to the gluon-gluon fusion contribution we show the contribution of the exclusive $pp \rightarrow pp f_0(980)$ process proceeding via the pomeron-pomeron fusion mechanism. The result is represented by the red dotted line. Here the calculation was made in the tensor-pomeron approach in the Born approximation (without absorptive corrections). Absorption corrections are important only when restricting to purely exclusive processes. For details regarding this approach we refer to [42–45]. In the calculation we take the pomeron-pomeron- $f_0(980)$ (PP $f_0(980)$) coupling parameters from [45], that is, $(g', g'') = (0.53, 2.67)$; see Table II of [45]. We have checked, that with these parameters we describe, within experimental errors, the cross sections reported very recently by the CMS Collaboration [46] for the exclusive $pp \rightarrow pp(f_0(980) \rightarrow \pi^+ \pi^-)$ process.

In the considered cases (gluon-gluon fusion) we observe relatively quick drop of $d\sigma/dp_t$ for $p_t \rightarrow 0$. Is it a specific feature of the considered UGDFs (JH or KMR)? In Fig. 6 we show the dominant TT contribution to $d\sigma/dp_t$ for other UGDFs used in the literature. In the left panel we show results for the GBW UGDF [47] (from CASCADE code) and the Kutak UGDF [48]. We have used two versions of the Kutak’s UGDF. Both introduce a hard scale dependence via a Sudakov form factor into solutions of a small- x evolution equation. The first version (linear) uses a BFKL evolution with a resummation of subleading terms. The second version (non-linear) uses an evolution equation of Balitsky-Kovchegov type. The non-linear version leads to smaller cross section, especially for small $f_0(980)$ meson transverse momenta. To better illustrate the dependence of UGDFs on q^2 in the right panel we present similar results with the Gaussian smearing of collinear GDF, often used in the context of TMDs, for different smearing parameter $\sigma_0 = 0.25, 0.5, 1.0$ GeV. The GJR08VFNS(LO) collinear GDF [49] was used for this purpose. As expected the shape of $d\sigma/dp_t$ strongly depends on the value of the smearing parameter σ_0 used in the calculation. The speed of approaching $d\sigma/dp_t$ for $p_t \rightarrow 0$ strongly depends on the value of σ_0 . It is impossible to describe simultaneously $p_t < 1$ GeV and $p_t > 1$ GeV regions with the same value of σ_0 . This illustrates the generic situation with all UGDFs.

The $d\sigma/dp_t \rightarrow 0$ for $p_t \rightarrow 0$ is related to the behavior of $\mathcal{F}_g(x, q^2, (\mu_F^2))$ for $q^2 \rightarrow 0$ because $q_1 + q_2 = p$. This nonperturbative part is rarely discussed by the UGDF

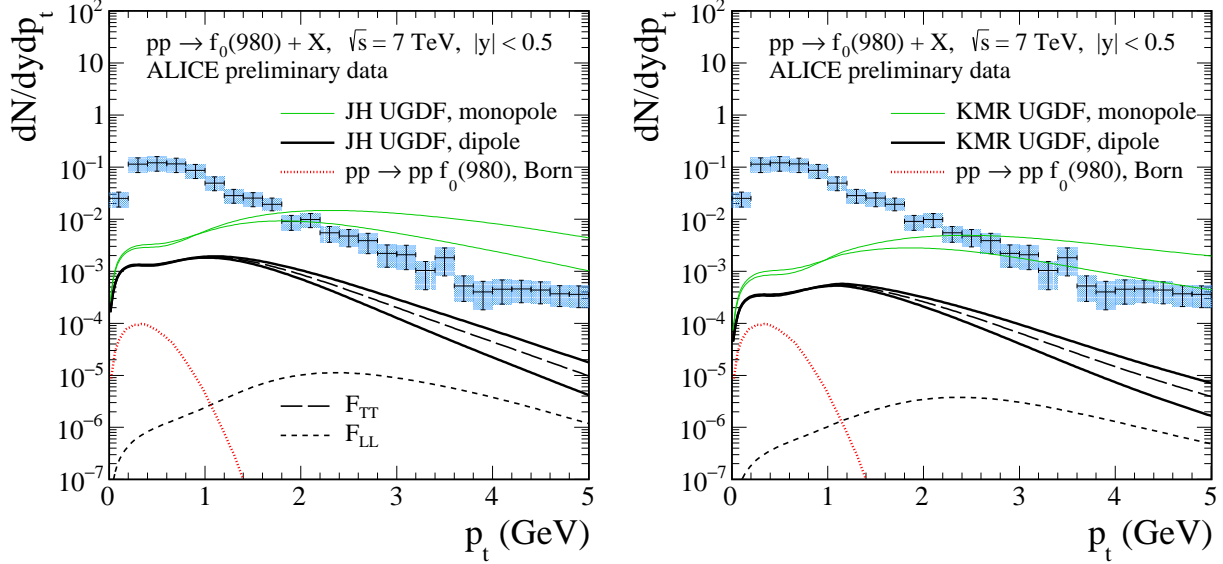


FIG. 5. The $f_0(980)$ meson transverse momentum distributions at $\sqrt{s} = 7$ TeV and $|y| < 0.5$. The preliminary ALICE data from [2] are shown for comparison. For the $g^*g^* \rightarrow f_0(980)$ contribution two different UGDFs are used: the JH (left panel) and KMR (right panel). Here, the $s\bar{s}$ flavor wave function of $f_0(980)$ is taken into account. Shown are TT and LL components in the amplitude and their coherent sum (total) for the monopole (green solid lines) and dipole (black solid lines) form factor parametrizations. In this calculation we used $\Lambda_M = \Lambda_D = m_{f_0}$ and $R_{LL/TT} = \pm 0.5$. The upper solid lines are for $R_{LL/TT} = -0.5$ while the bottom solid lines for 0.5. The dotted line corresponds to the Born-level result for the $pp \rightarrow pp f_0(980)$ process via pomeron-pomeron fusion.

builders and is often done by an extrapolation from the perturbative region of $q^2 > (0.5 - 1.0) \text{ GeV}^2$, trying to satisfy:

$$\int^{\mu_F^2} dq^2 \mathcal{F}_g(x, q^2, (\mu_F^2)) \sim xg(x, \mu_F^2), \quad (3.4)$$

or trying to describe deep-inelastic scattering data, especially from HERA. Above $g(x, \mu^2)$ is the collinear GDF.

Such a procedure(s) is (are) of course not unique. To illustrate how differently it is done for different UGDFs in Fig. 7 we present a few examples of $d^2\sigma/dq_{1t}dq_{2t}$ for the JH, KMR, GBW, and Kutak (non-linear) UGDFs. The maximal contributions, even to the p_t -integrated cross section come from the region of rather small gluon transverse momenta $q_{1t}, q_{2t} < 1$ GeV. This is domain of nonperturbative physics which is not fully under control. The GBW UGDF was destined for this region. On the other hand the larger- p_t region ($p_t > 2$ GeV) is sensitive to $q_{1t}, q_{2t} > 1$ GeV where perturbative methods apply. The fault visible at $q_{1t} + q_{2t} = 6$ GeV for some distributions is due to limit of integration over p_t to $p_t \in (0, 6)$ GeV. The sudden drop of the cross sections for the Kutak UGDF for $q_{1t} < 0.4$ GeV or $q_{2t} < 0.4$ GeV is of purely technical nature and comes from the limited grid in gluon transverse momentum which was available to us. We decided not to make extra efforts to extrapolate the grids down to zero.

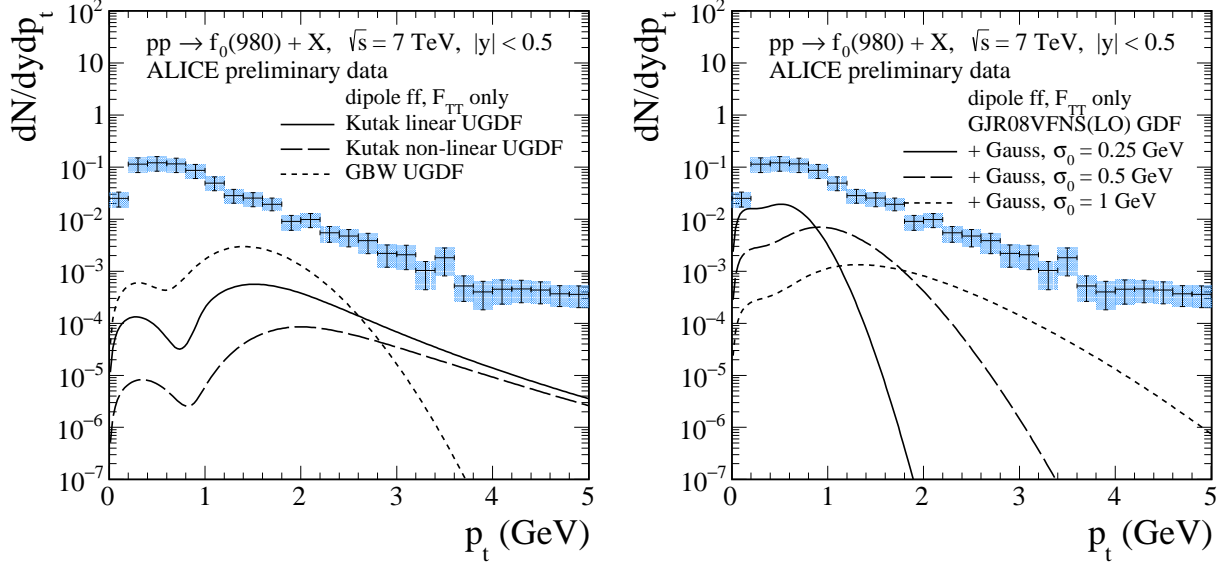


FIG. 6. Transverse momentum distribution of $f_0(980)$ for different UGDFs from the literature. In the left panel we show the results for Kutak linear (solid line), Kutak non-linear (long-dashed line) and GBW (dotted line) UGDFs. In the right panel we present our study of the dependence on the Gaussian smearing parameter σ_0 . Here GJR08VFNS(LO) GDF [49] was used.

It is too risky, in our opinion, to use the $d\sigma/dp_t$ data for $f_0(980)$ production to model UGDFs, as it is improbable that the $g^*g^* \rightarrow f_0(980)$ is the only one. In addition, the result for $d\sigma/dp_t$ strongly depends on the assumption done for the flavor structure of $f_0(980)$ as discussed above. It is not excluded that production of other light/heavy mesons for small p_t can be used to constrain $\mathcal{F}_g(x, q^2, (\mu_F^2))$ at small q^2 .

Below we shall consider also color octet contribution calculated in the color evaporation approach.

B. Color evaporation model (CEM)

In the present study the cross sections for $u\bar{u}$ and $d\bar{d}$ or alternatively $s\bar{s}$ minijet pair production are calculated in the k_t -factorization approach or in the collinear approach. In both cases the calculations are done with the help of the KaTie Monte Carlo code [50]. Considering production of (soft) minijets a real problem is a regularization of the cross section at small transverse momenta. Here we follow the methods adopted for collinear approach in PYTHIA and multiply the calculated cross section by a somewhat arbitrary suppression factor:

$$F_{\text{sup}}(p_t) = \frac{p_t^4}{((p_t^0)^2 + p_t^2)^2}, \quad (3.5)$$

where p_t^0 is a free parameter of the model. In the following calculations we take different values of p_t^0 , in order to show sensitivity of the results to the choice of this parameter. The parameter goes also into the argument of the strong coupling constant $\alpha_s(\mu_R^2) = \alpha_s((p_t^0)^2 + p_t^2)$.

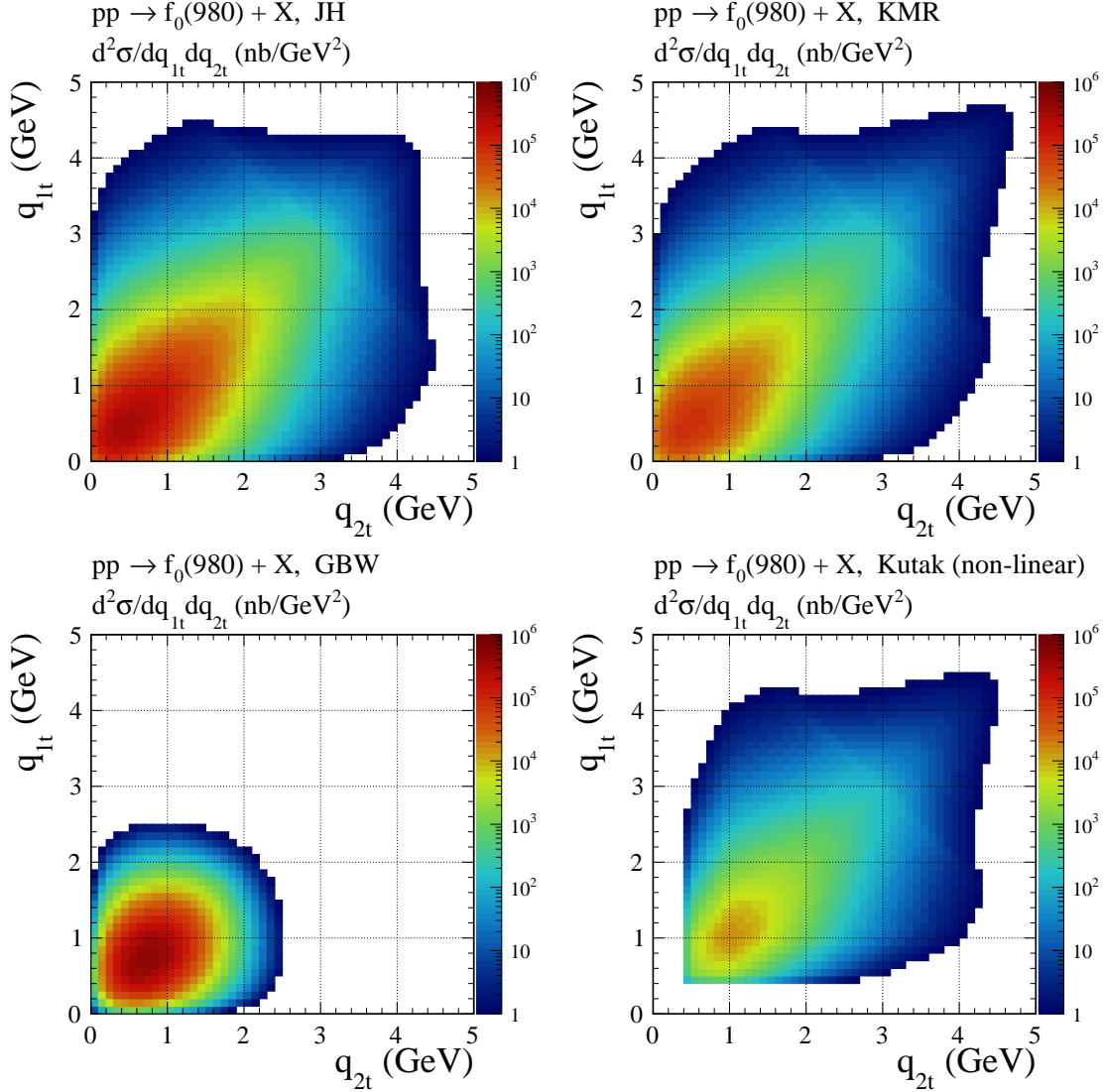


FIG. 7. Two-dimensional distributions in gluon transverse momenta for different UGDs from the literature.

1. The k_t -factorization approach to CEM with the KMR UPDFs

In the k_t -factorization approach the non-zero $q\bar{q}$ pair transverse momentum can be generated even at leading-order when only the $2 \rightarrow 2$ three-level partonic processes are taken into account. Here we include both the gg -fusion and $q\bar{q}$ -annihilation mechanisms. By applying the KMR UPDFs one effectively includes a part of real higher order corrections. Large amount of extra hard emissions present in this model may lead to large transverse momentum of the produced system, without any additional emissions at the level of hard matrix elements.

Technically, in the numerical calculations here, the suppression factor includes the fact that the transverse momenta of outgoing minijets are not balanced and it takes the fol-

lowing form:

$$F_{\text{sup}}^{(2)}(p_{1t}^2, p_{2t}^2) = \frac{p_{1t}^2}{(p_t^0)^2 + p_{1t}^2} \times \frac{p_{2t}^2}{(p_t^0)^2 + p_{2t}^2}. \quad (3.6)$$

The KaTie Monte Carlo generator does not have any problems with the generation of the events in the case of the $2 \rightarrow 2$ processes, even if there is no additional cut-off on the outgoing minijets transverse momenta (thus low- p_t cuts are not necessary here). The generated events for massless quarks/antiquarks are weighted by the suppression factor (3.6).

In Fig. 8 we show the results for different values of p_t^0 in (3.6), that is, $p_t^0 = 0.01, 0.5,$ and 1.0 GeV. Large damping of the $q\bar{q}$ -pair p_t distributions is visible. In the following, we choose $p_t^0 = 0.01$ GeV.

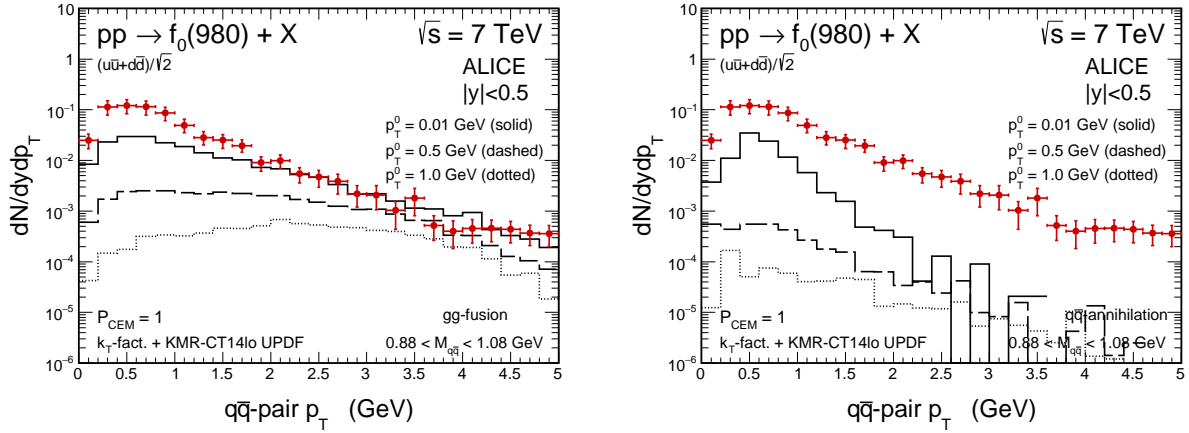


FIG. 8. The transverse momentum distribution of $f_0(980)$ for the KMR-CT14lo UPDFs for different p_t^0 in (3.6) for the gg -fusion (left) and $q\bar{q}$ (right) mechanisms. The calculations were done for $M_{q\bar{q}} \in (0.88, 1.08)$ GeV.

As can be seen from Fig. 9 we obtain a good description of the ALICE data even with the leading-order $2 \rightarrow 2$ mechanisms only. In the top panels of Fig. 9 we show results for the first $\frac{1}{\sqrt{2}}(|u\bar{u}\rangle + |d\bar{d}\rangle)$ scenario (2.12) while in the bottom panels of Fig. 9 for the $|s\bar{s}\rangle$ scenario (2.13). We show also the dependence of the final results on the collinear parton distributions used to the calculation of the KMR UPDFs. The results in the left panels correspond to the CT14lo PDF [51] while in the right panels to the MMHT2014lo PDF [52]. The differences at so small scales between different collinear PDFs could be significant. Here and in the following the shaded bands represents uncertainties of the calculations related to renormalization scale chosen as an argument in strong coupling α_s . We vary the μ_R over the central value, which is set to be averaged transverse mass of outgoing particles, by factor 2.

Since the assumption of $\frac{1}{\sqrt{2}}(|u\bar{u}\rangle + |d\bar{d}\rangle)$ for the flavor wave function of $f_0(980)$ may be not realistic we consider also the $s\bar{s}$ scenario as was done for color-singlet gluon-gluon fusion. It is obvious that the corresponding cross section will be smaller than that for the light $q\bar{q}$ scenario. In the right bottom panel of Fig. 9 we show corresponding results for the

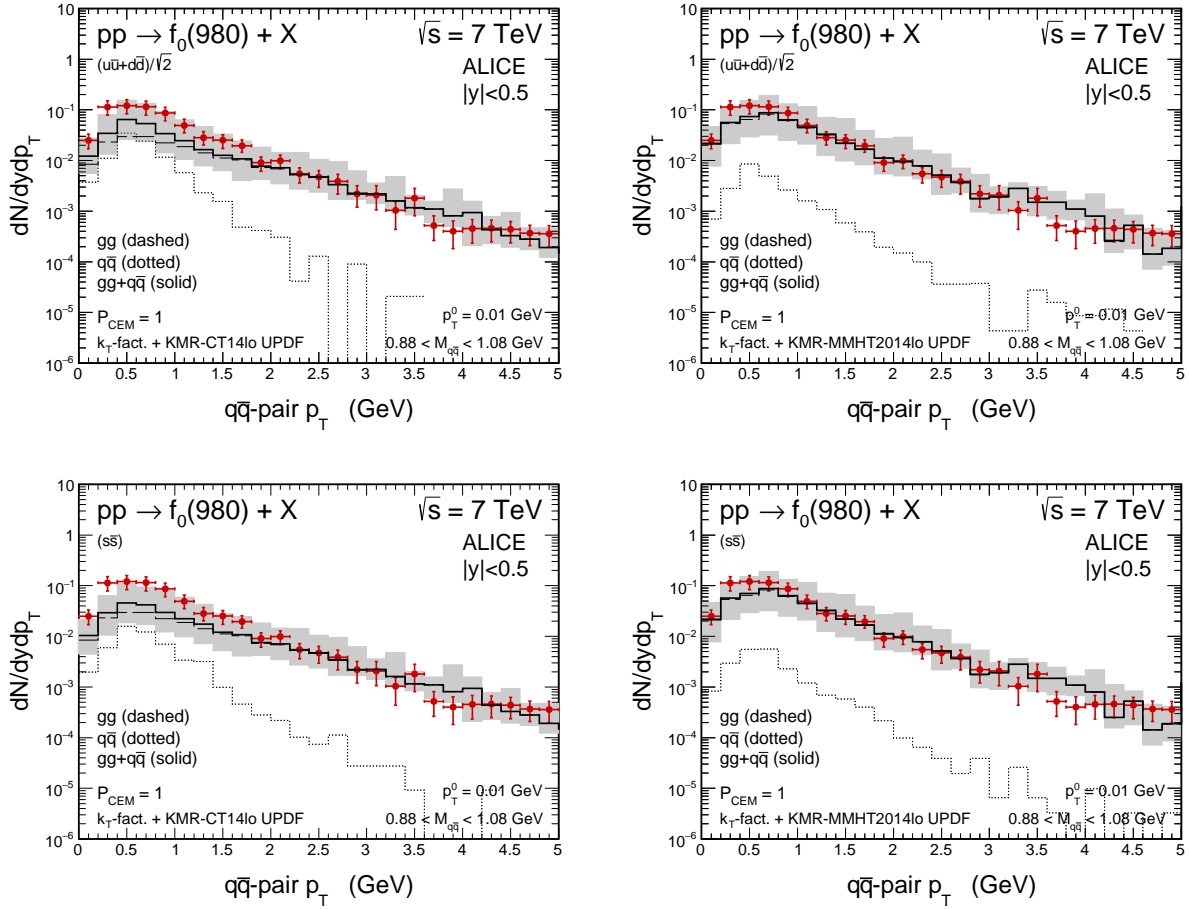


FIG. 9. The $f_0(980)$ meson transverse momentum distributions at $\sqrt{s} = 7$ TeV and $|y| < 0.5$ calculated in the color evaporation model based on the k_t -factorization approach using the KMR-CT14lo (left) and KMR-MMHT2014lo (right) UPDFs together with the preliminary ALICE data from [2]. The calculations were done in quark-antiquark invariant mass region $M_{q\bar{q}} \in (0.88, 1.08)$ GeV for the light $q\bar{q}$ scenario (2.12) (see the top panels) and for the $s\bar{s}$ scenario (2.13) (see the bottom panels). The results for the gg -fusion and $q\bar{q}$ mechanisms are shown separately. Their sum is shown by the solid line. Here we used extremely small $p_t^0 = 0.01$ GeV in (3.6).

$s\bar{s}$ scenario. It is obvious that here (KMR-MMHT2014lo UPDF) the $g^*g^* \rightarrow s\bar{s} \rightarrow f_0(980)$ is the dominant mechanism. Assuming massless s and \bar{s} the corresponding cross section is very similar as for $\frac{1}{\sqrt{2}}(u\bar{u} + d\bar{d})$ scenario because for high-energy collisions the gluon-gluon fusion is the dominant contribution.

The calculations done so far were performed for massless quarks/antiquarks. How important is the quark/antiquark mass for our k_t -factorization results is illustrated in Fig. 10. Here we show $M_{q\bar{q}}$ invariant mass distributions for three different quark masses: $m_q = 0$ GeV (with the extra regularization procedure given by Eq. (3.6), $p_t^0 = 0.01$ GeV), $m_q = 0.1$ GeV (current s/\bar{s} mass), $m_q = 0.3$ GeV (constituent light quark (u, d) masses). We show also the window of $M_{q\bar{q}}$ selected for the $f_0(980)$ meson, used in the color-evaporation model calculations; see Eq. (2.16). For finite quark/antiquark masses no extra regularization is needed. There is no strong dependence on m_q provided it is not

too big. For instance for $m_q \approx 0.5$ GeV, the s quark constituent mass, the cross section for the color evaporation model vanishes when $M_{q\bar{q}} > m_{f_0}$.

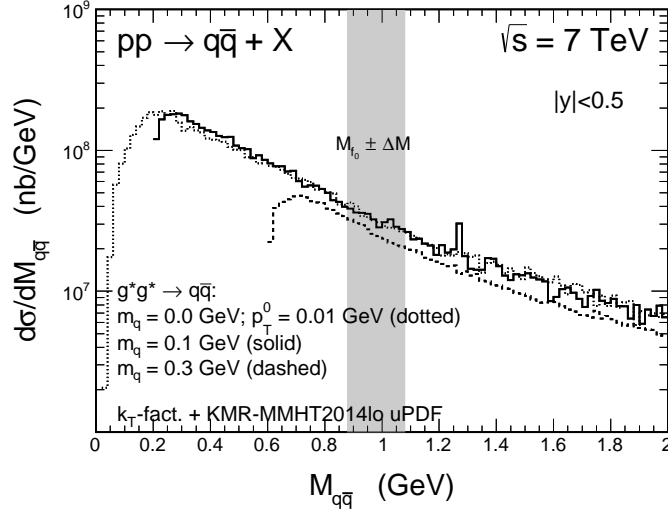


FIG. 10. $M_{q\bar{q}}$ invariant mass distribution for three different quark/antiquark masses specified in the legend of the figure.

In Fig. 11 we show transverse momentum distribution for the $g^*g^* \rightarrow q\bar{q}$ and $q^*\bar{q}^* \rightarrow q\bar{q}$ mechanisms added together for different final state quark/antiquark masses: 0.1, 0.3 GeV. Technically, we use here off-shell matrix elements derived for heavy quark production including both the gg -fusion and light quark $q\bar{q}$ -annihilation into heavy (massive) quark-antiquark pair. We conclude that the results do not depend too much on the mass of produced quark/antiquark.

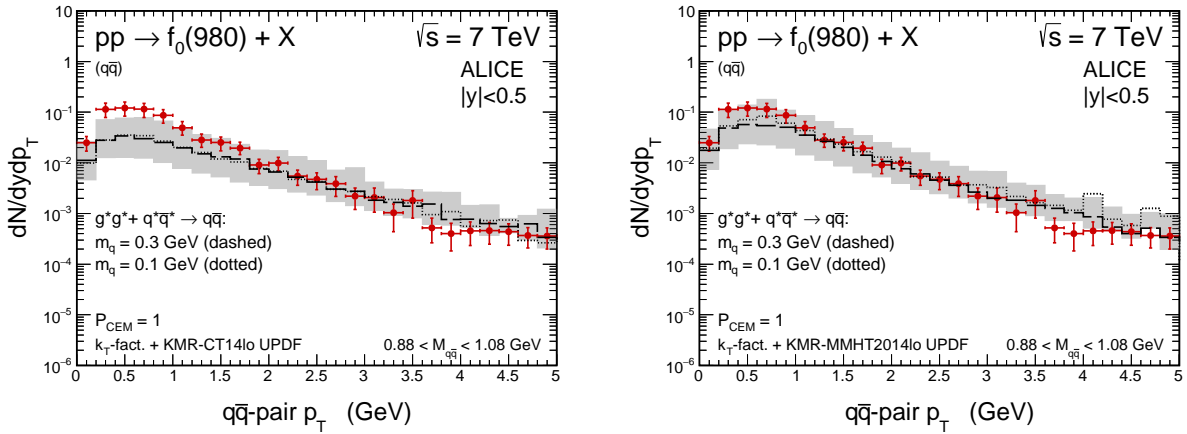


FIG. 11. The transverse momentum distributions of $f_0(980)$ for the KMR UPDFs for two masses of produced quark/antiquark: $m_q = 0.1$ GeV (dotted) and $m_q = 0.3$ GeV (dashed). The calculations were done in the $q\bar{q}$ invariant mass region $M_{q\bar{q}} \in (0.88, 1.08)$ GeV.

2. *The collinear approach to CEM with the 2 → 3 tree-level partonic processes*

In the collinear approach the non-zero $q\bar{q}$ pair transverse momentum can be generated only beyond the leading-order approximation. In the calculations we take into account the 2 → 3 partonic processes at the tree-level. So here the $q\bar{q}$ -pair is associated with extra gluon or quark which comes from the hard matrix elements. Here we include all the partonic subprocesses with gg -, qg - and $q\bar{q}$ -types of initial states. The full list of the processes included is shown below:

- gg -fusion:
 $gg \rightarrow gu\bar{u}, gg \rightarrow gdd\bar{d}$
- qg -interaction:
 $gu \rightarrow uu\bar{u}, gd \rightarrow du\bar{u}, gs \rightarrow su\bar{u}, g\bar{u} \rightarrow \bar{u}u\bar{u}, g\bar{d} \rightarrow \bar{d}u\bar{u}, g\bar{s} \rightarrow \bar{s}u\bar{u}, ug \rightarrow uu\bar{u},$
 $dg \rightarrow du\bar{u}, sg \rightarrow su\bar{u}, \bar{u}g \rightarrow \bar{u}u\bar{u}, \bar{d}g \rightarrow \bar{d}u\bar{u}, \bar{s}g \rightarrow \bar{s}u\bar{u}, gu \rightarrow udd\bar{d}, gd \rightarrow ddd\bar{d},$
 $gs \rightarrow sdd\bar{d}, g\bar{u} \rightarrow \bar{u}dd\bar{d}, g\bar{d} \rightarrow \bar{d}dd\bar{d}, g\bar{s} \rightarrow \bar{s}dd\bar{d}, ug \rightarrow udd\bar{d}, dg \rightarrow ddd\bar{d}, sg \rightarrow sdd\bar{d},$
 $\bar{u}g \rightarrow \bar{u}dd\bar{d}, \bar{d}g \rightarrow \bar{d}dd\bar{d}, \bar{s}g \rightarrow \bar{s}dd\bar{d}$
- $q\bar{q}$ -annihilation:
 $u\bar{u} \rightarrow gu\bar{u}, d\bar{d} \rightarrow gu\bar{u}, s\bar{s} \rightarrow gu\bar{u}, \bar{u}u \rightarrow gu\bar{u}, \bar{d}d \rightarrow gu\bar{u}, \bar{s}s \rightarrow gu\bar{u}, d\bar{d} \rightarrow gdd\bar{d},$
 $u\bar{u} \rightarrow gdd\bar{d}, s\bar{s} \rightarrow gdd\bar{d}, \bar{d}d \rightarrow gdd\bar{d}, \bar{u}u \rightarrow gdd\bar{d}, \bar{s}s \rightarrow gdd\bar{d}$

In the case of the collinear calculations of the 2 → 3 processes the suppression factor takes the following form:

$$\Gamma_{\text{sup}}^{(3)}(p_{1t}^2, p_{2t}^2, p_{3t}^2) = \frac{p_{1t}^2}{(p_t^0)^2 + p_{1t}^2} \times \frac{p_{2t}^2}{(p_t^0)^2 + p_{2t}^2} \times \frac{p_{3t}^2}{(p_t^0)^2 + p_{3t}^2}. \quad (3.7)$$

The final results that correspond to the collinear approach are shown in Fig. 12. Again, here we need to check sensitivity of the results related to the choice of the collinear PDFs. In the left panel we show results for the CT14lo PDF while in the right panel for the MMHT2014lo PDF.

Clearly, quite different behavior of the calculated distributions at small transverse momenta is obtained when comparing the results of the k_t -factorization and leading-order collinear approach for the pair transverse momentum distribution. In the k_t -factorization approach the cross section at very small transverse momenta goes down to zero, which is not the case of the collinear calculations. This difference has a purely kinematical origin and appears as a result of exact treatment of the kinematics with no approximations in the k_t -factorization approach. Similar effect was discussed e.g. in Ref. [53] in the case of dijet production.

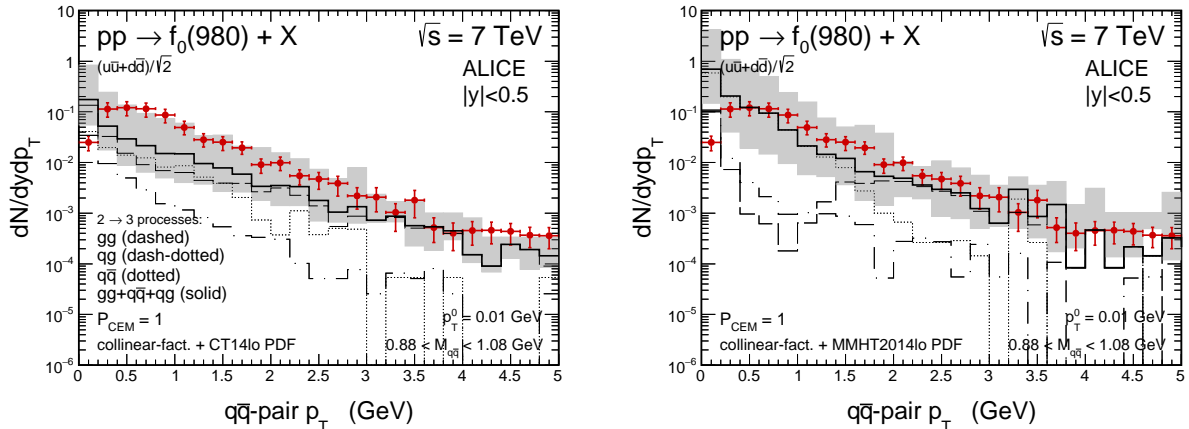


FIG. 12. The $f_0(980)$ meson transverse momentum distributions at $\sqrt{s} = 7$ TeV and $|y| < 0.5$, calculated in the color evaporation model based on the collinear approach, using the CT14lo (left) and MMHT2014lo (right) PDFs together with the preliminary ALICE data from [2]. The calculations were done in quark-antiquark invariant mass region $M_{q\bar{q}} \in (0.88, 1.08)$ GeV. Here the gg , qg and $q\bar{q}$ induced interaction mechanisms are shown separately. Shown are results for the light $q\bar{q}$ scenario (2.12) for the flavor wave function of $f_0(980)$. In the calculations we used $p_t^0 = 0.01$ GeV in (3.7).

IV. CONCLUSIONS

In this letter we have presented a first exploratory calculation of inclusive $f_0(980)$ meson production at the LHC energies. Two different mechanisms have been considered. The first mechanism is the color-singlet gluon-gluon fusion known to give a rather good description of the η_c and χ_c production [26, 28]. The second is the color evaporation model used e.g. to describe the production of J/ψ meson [31]. The results have been compared to preliminary ALICE data [2].

We have started our analysis by considering the $\gamma^*\gamma^* \rightarrow f_0(980)$ coupling. Unlike for charmonia we have taken a more phenomenological approach. The general structure of the $\gamma^*\gamma^* \rightarrow f_0$ and $g^*g^* \rightarrow f_0$ vertices were known from the literature. However, the corresponding form factors for $g^*g^* \rightarrow f_0(980)$ are rather poorly known. The $F_{TT}(0,0)$ has been fixed based on the formula for $\Gamma(f_0(980) \rightarrow \gamma\gamma)$; see Eq. (2.3). $F_{LL}(Q_1^2, Q_2^2)$ for $f_0(980)$ is rather unknown and in principle a model of the $f_0(980)$ wave function is needed. In the present analysis we have parametrized the $F_{LL}(Q_1^2, Q_2^2)$ form factor in analogy to the results obtained recently from a microscopic calculation for χ_{c0} [26]. The parametrizations for $F_{TT/LL}(Q_1^2, Q_2^2)$ were restricted only to some extent by the Belle data for the $e^+e^- \rightarrow e^+e^-\pi\pi$ reactions [54, 55].

Then the $g^*g^* \rightarrow f_0(980)$ coupling has been obtained by replacing electromagnetic coupling constant by strong coupling constant and by modifying relevant color factors.

The contribution of color-singlet gluon-gluon fusion strongly depends on the assumed flavor structure of the $f_0(980)$ meson. For instance result for the $s\bar{s}$ scenario (2.13) is almost an order of magnitude larger than that for the light $q\bar{q}$ scenario (2.12). Large gluonic component in the $f_0(980)$ meson would further increase the cross section for color-flavor component.

The results for hadroproduction depend on $g^*g^* \rightarrow f_0(980)$ form factors F_{TT} and F_{LL} that have been parametrized in the present paper; see Eqs. (2.5)–(2.8). With a plausible parametrization one can almost understand transverse momentum distribution of $f_0(980)$ at $p_t > 3$ GeV in the $s\bar{s}$ scenario, but the results for the light quark/antiquark scenario is much below the data for $p_t < 2$ GeV. Clearly a different mechanism is needed to describe the region of small transverse momenta of $f_0(980)$. The light $q\bar{q}$ scenario gives result much below the ALICE data.

In the present paper we have considered also color evaporation mechanism. Also the color evaporation cross sections have been calculated in the k_t -factorization approach, as done recently for J/ψ production. The KMR unintegrated parton distribution functions (both for gluons, quarks, and antiquarks) have been used in this context. Many different processes leading to $u\bar{u}$, $d\bar{d}$ or $s\bar{s}$ final states have been considered. We have done also similar calculations at collinear NLO tree-level partonic approach. Some regularization procedure has been used in both cases. Both the k_t -factorization and the collinear NLO approaches lead to rather similar results.

We have shown that the results for color-singlet fusion, constrained by the $\gamma\gamma \rightarrow f_0(980)$ form factor at the on-shell point $|F_{TT}(0,0)|$, strongly depends on the assumed flavor structure of $f_0(980)$. Assuming $u\bar{u} + d\bar{d}$ flavor structure leads to negligible contribution of the color-singlet gluon-gluon fusion mechanism. Assuming $s\bar{s}$ flavor structure (more realistic in our opinion) gives the contribution which may be important at $p_t > 3$ GeV. In contrast, the color evaporation mechanism is much less sensitive to the flavor structure.

We conclude that the color-singlet gluon-gluon fusion is not able to describe the preliminary ALICE data [2] in the whole range of transverse momenta. The color evaporation model nicely describes the shape of transverse momentum distribution. To describe absolute normalization rather maximal probabilities ($P_{\text{CEM}} = 1$) must be used. It seems too early to draw definite conclusion. More global picture may arise by analysis of production of other isoscalar mesons (such as $\eta, \eta', f_2(1270), f_1(1285)$, etc.). This clearly goes beyond the scope of the present analysis.

We have calculated also $\mathbb{P}\mathbb{P} \rightarrow f_0(980)$ fusion contribution and found nonnegligible but small contribution. This contribution is concentrated at rather small $f_0(980)$ transverse momenta ($p_t < 2$ GeV) but its role is rather marginal.

ACKNOWLEDGMENTS

A.S. is indebted to Wolfgang Schäfer for a collaboration on quarkonium production and a discussion on related issues. This study was partially supported by the Polish National Science Centre under grant No. 2018/31/B/ST2/03537 and by the Center for Innovation and Transfer of Natural Sciences and Engineering Knowledge in Rzeszów (Poland).

[1] P. Lebedowicz, R. Maciuła, and A. Szczurek, a paper in preparation.

- [2] G. R. Lee, Ph.D. thesis, *Resonance production in the $\pi^+\pi^-$ decay channel in proton-proton collisions at 7 TeV*, University of Birmingham, June 6, 2016. http://www.hep.ph.bham.ac.uk/publications/thesis/grl_thesis.pdf.
- [3] F. E. Close and N. A. Törnqvist, *Scalar mesons above and below 1 GeV*, J. Phys. **G28** (2002) R249, arXiv:hep-ph/0204205 [hep-ph].
- [4] L. Maiani, F. Piccinini, A. D. Polosa, and V. Riquer, *New Look at Scalar Mesons*, Phys. Rev. Lett. **93** (2004) 212002, arXiv:hep-ph/0407017 [hep-ph].
- [5] N. A. Törnqvist, *Understanding the scalar meson $q\bar{q}$ nonet*, Z. Phys. **C68** (1995) 647, arXiv:hep-ph/9504372 [hep-ph].
- [6] M. Boglione and M. R. Pennington, *Dynamical generation of scalar mesons*, Phys. Rev. **D65** (2002) 114010, arXiv:hep-ph/0203149 [hep-ph].
- [7] R. L. Jaffe, *Multiquark hadrons. I. Phenomenology of $Q^2\bar{Q}^2$ mesons*, Phys. Rev. **D15** (1977) 267.
- [8] R. L. Jaffe, *Multiquark hadrons. II. Methods*, Phys. Rev. **D15** (1977) 281.
- [9] J. D. Weinstein and N. Isgur, *Do Multiquark Hadrons Exist?*, Phys. Rev. Lett. **48** (1982) 659.
- [10] J. D. Weinstein and N. Isgur, *$qq\bar{q}\bar{q}$ system in a potential model*, Phys. Rev. **D27** (1983) 588.
- [11] J. D. Weinstein and N. Isgur, *$K\bar{K}$ molecules*, Phys. Rev. **D41** (1990) 2236.
- [12] V. Baru, J. Haidenbauer, C. Hanhart, Yu. Kalashnikova, and A. E. Kudryavtsev, *Evidence that the $a_0(980)$ and $f_0(980)$ are not elementary particles*, Phys. Lett. **B586** (2004) 53, arXiv:hep-ph/0308129 [hep-ph].
- [13] G. 't Hooft, G. Isidori, L. Maiani, A. D. Polosa, and V. Riquer, *A theory of scalar mesons*, Phys. Lett. **B662** (2008) 424, arXiv:0801.2288 [hep-ph].
- [14] R. Fleischer, R. Knecht, and G. Ricciardi, *Anatomy of $B_{s,d}^0 \rightarrow J/\psi f_0(980)$* , Eur. Phys. J. **C71** (2011) 1832, arXiv:1109.1112 [hep-ph].
- [15] L. Maiani, A. D. Polosa, and V. Riquer, *Structure of light scalar mesons from D_s and D^0 non-leptonic decays*, Phys. Lett. **B651** (2007) 129, arXiv:hep-ph/0703272 [hep-ph].
- [16] H.-Y. Cheng, C.-K. Chua, and K.-C. Yang, *Charmless hadronic B decays involving scalar mesons: Implications to the nature of light scalar mesons*, Phys. Rev. **D73** (2006) 014017, arXiv:hep-ph/0508104 [hep-ph].
- [17] S. Stone and L. Zhang, *Use of $B \rightarrow J/\psi f_0$ Decays to Discern the $q\bar{q}$ or Tetraquark Nature of Scalar Mesons*, Phys. Rev. Lett. **111** no. 6, (2013) 062001, arXiv:1305.6554 [hep-ex].
- [18] M. Tanabashi *et al.*, (Particle Data Group), *Review of Particle Physics*, Phys. Rev. **D98** no. 3, (2018) 030001.
- [19] R. Aaij *et al.*, (LHCb Collaboration), *Measurement of the resonant and CP components in $\bar{B}^0 \rightarrow J/\psi\pi^+\pi^-$ decays*, Phys. Rev. **D90** no. 1, (2014) 012003, arXiv:1404.5673 [hep-ex].
- [20] V. Pauk and M. Vanderhaeghen, *Single meson contributions to the muon's anomalous magnetic moment*, Eur. Phys. J. **C74** no. 8, (2014) 3008, arXiv:1401.0832 [hep-ph].
- [21] G. Colangelo, M. Hoferichter, M. Procura, and P. Stoffer, *Dispersive approach to hadronic light-by-light scattering*, JHEP **09** (2014) 091, arXiv:1402.7081 [hep-ph].
- [22] A. E. Dorokhov, A. E. Radzhabov, and A. S. Zhevlakov, *Dynamical quark loop light-by-light contribution to muon $g-2$ within the nonlocal chiral quark model*, Eur. Phys. J. **C75** no. 9, (2015) 417, arXiv:1502.04487 [hep-ph].
- [23] F. De Fazio and M. R. Pennington, *Probing the structure of $f_0(980)$ through radiative ϕ decays*, Phys. Lett. **B521** (2001) 15, arXiv:hep-ph/0104289 [hep-ph].
- [24] P. Kroll, *A study of the $\gamma^* - f_0(980)$ transition form factors*, Eur. Phys. J. **C77** no. 2, (2017) 95, arXiv:1610.01020 [hep-ph].

- [25] V. Pascalutsa, V. Pauk, and M. Vanderhaeghen, *Light-by-light scattering sum rules constraining meson transition form factors*, Phys. Rev. **D85** (2012) 116001, arXiv:1204.0740 [hep-ph].
- [26] I. Babiarz, R. Pasechnik, W. Schäfer, and A. Szczurek, *Hadroproduction of scalar P-wave quarkonia in the light-front k_T -factorization approach*, arXiv:2002.09352 [hep-ph].
- [27] A. Cisek and A. Szczurek, *Prompt inclusive production of J/ψ , ψ' and χ_c mesons at the LHC in forward directions within the NRQCD k_t -factorization approach: Search for the onset of gluon saturation*, Phys. Rev. **D97** no. 3, (2018) 034035, arXiv:1712.07943 [hep-ph].
- [28] I. Babiarz, R. Pasechnik, W. Schäfer, and A. Szczurek, *Prompt hadroproduction of $\eta_c(1S, 2S)$ in the k_T -factorization approach*, JHEP **02** (2020) 037, arXiv:1911.03403 [hep-ph].
- [29] H. Fritzsche, *Producing heavy quark flavors in hadronic collisions: A test of quantum chromodynamics*, Phys. Lett. **B67** (1977) 217.
- [30] F. Halzen, *CVC for gluons and hadroproduction of quark flavors*, Phys. Lett. **B69** (1977) 105.
- [31] R. Maciuła, A. Szczurek, and A. Cisek, *J/ψ -meson production within improved color evaporation model with the k_T -factorization approach for $c\bar{c}$ production*, Phys. Rev. **D99** no. 5, (2019) 054014, arXiv:1810.08063 [hep-ph].
- [32] G. Antchev *et al.*, (TOTEM Collaboration), *Measurement of proton-proton elastic scattering and total cross-section at $\sqrt{s} = 7$ TeV*, EPL **101** no. 2, (2013) 21002.
- [33] G. Aad *et al.*, (ATLAS Collaboration), *Measurement of the total cross section from elastic scattering in pp collisions at $\sqrt{s} = 7$ TeV with the ATLAS detector*, Nucl. Phys. **B889** (2014) 486, arXiv:1408.5778 [hep-ex].
- [34] H. Jung *et al.*, *The CCFM Monte Carlo generator CASCADE version 2.2.03*, Eur. Phys. J. **C70** (2010) 1237, arXiv:1008.0152 [hep-ph].
- [35] M. A. Kimber, A. D. Martin, and M. G. Ryskin, *Unintegrated parton distributions*, Phys. Rev. **D63** (2001) 114027, arXiv:hep-ph/0101348 [hep-ph].
- [36] G. Watt, A. D. Martin, and M. G. Ryskin, *Unintegrated parton distributions and electroweak boson production at hadron colliders*, Phys. Rev. **D70** (2004) 014012, arXiv:hep-ph/0309096 [hep-ph]. [Erratum: Phys. Rev.D70,079902(2004)].
- [37] A. D. Martin, M. G. Ryskin, and G. Watt, *NLO prescription for unintegrated parton distributions*, Eur. Phys. J. **C66** (2010) 163, arXiv:0909.5529 [hep-ph].
- [38] F. Hautmann and H. Jung, *Transverse momentum dependent gluon density from DIS precision data*, Nucl. Phys. **B883** (2014) 1, arXiv:1312.7875 [hep-ph].
- [39] M. Ciafaloni, *Coherence effects in initial jets at small Q^2/s* , Nucl. Phys. **B296** (1988) 49.
- [40] S. Catani, F. Fiorani, and G. Marchesini, *QCD coherence in initial state radiation*, Phys. Lett. **B234** (1990) 339.
- [41] S. Catani, F. Fiorani, and G. Marchesini, *Small- x behavior of initial state radiation in perturbative QCD*, Nucl. Phys. **B336** (1990) 18.
- [42] C. Ewerz, M. Maniatis, and O. Nachtmann, *A Model for Soft High-Energy Scattering: Tensor Pomeron and Vector Odderon*, Annals Phys. **342** (2014) 31, arXiv:1309.3478 [hep-ph].
- [43] P. Lebiedowicz, O. Nachtmann, and A. Szczurek, *Exclusive central diffractive production of scalar and pseudoscalar mesons; tensorial vs. vectorial pomeron*, Annals Phys. **344** (2014) 301, arXiv:1309.3913 [hep-ph].
- [44] P. Lebiedowicz, O. Nachtmann, and A. Szczurek, *Central exclusive diffractive production of the $\pi^+\pi^-$ continuum, scalar, and tensor resonances in pp and $p\bar{p}$ scattering within the tensor Pomeron approach*, Phys. Rev. **D93** (2016) 054015, arXiv:1601.04537 [hep-ph].
- [45] P. Lebiedowicz, O. Nachtmann, and A. Szczurek, *Towards a complete study of central exclusive production of K^+K^- pairs in proton-proton collisions within the tensor Pomeron approach*,

- Phys. Rev. **D98** (2018) 014001, arXiv:1804.04706 [hep-ph].
- [46] A. M. Sirunyan *et al.*, (CMS Collaboration), *Study of central exclusive $\pi^+\pi^-$ production in proton-proton collisions at $\sqrt{s} = 5.02$ and 13 TeV*, CMS-FSQ-16-006, CERN-EP-2020-005, arXiv:2003.02811 [hep-ex].
- [47] K. J. Golec-Biernat and M. Wusthoff, *Diffraction parton distributions from the saturation model*, Eur. Phys. J. **C20** (2001) 313, arXiv:hep-ph/0102093 [hep-ph].
- [48] K. Kutak, *Hard scale dependent gluon density, saturation and forward-forward dijet production at the LHC*, Phys. Rev. **D91** (2015) 034021, arXiv:1409.3822 [hep-ph].
- [49] M. Glück, P. Jimenez-Delgado, E. Reya, and C. Schuck, *On the role of heavy flavor parton distributions at high energy colliders*, Phys.Lett. **B664** (2008) 133, arXiv:0801.3618 [hep-ph].
- [50] A. van Hameren, *KaTie: For parton-level event generation with k_T -dependent initial states*, Comput. Phys. Commun. **224** (2018) 371, arXiv:1611.00680 [hep-ph].
- [51] S. Dulat, T.-J. Hou, J. Gao, M. Guzzi, J. Huston, P. Nadolsky, J. Pumplin, C. Schmidt, D. Stump, and C. P. Yuan, *New parton distribution functions from a global analysis of quantum chromodynamics*, Phys. Rev. **D93** no. 3, (2016) 033006, arXiv:1506.07443 [hep-ph].
- [52] L. A. Harland-Lang, A. D. Martin, P. Motylinski, and R. S. Thorne, *Parton distributions in the LHC era: MMHT 2014 PDFs*, Eur. Phys. J. **C75** no. 5, (2015) 204, arXiv:1412.3989 [hep-ph].
- [53] K. Kutak, R. Maciula, M. Serino, A. Szczurek and A. van Hameren, *Four-jet production in single- and double-parton scattering within high-energy factorization*, JHEP **04** (2016) 175, arXiv:1602.06814 [hep-ph].
- [54] T. Mori *et al.*, (Belle Collaboration), *High statistics study of the $f_0(980)$ resonance in $\gamma\gamma \rightarrow \pi^+\pi^-$ production*, Phys. Rev. **D75** (2007) 051101, arXiv:hep-ex/0610038 [hep-ex].
- [55] S. Uehara *et al.*, (Belle Collaboration), *High-statistics measurement of neutral-pion pair production in two-photon collisions*, Phys. Rev. **D78** (2008) 052004, arXiv:0805.3387 [hep-ex].